DAMAGE THRESHOLD STUDIES OF GLASS LASER MATERIALS

N. L. Boling, et al

Owens-Illinois, Incorporated

Prepared for:

Advanced Research Projects Agency

30 June 1972

A REPORT FROM

OWENS-ILLINOIS TECHNICAL CENTER

FORM NO. 605-K

CONSUMER & TECHNICAL PRODUCTS DIVISION
RESEARCH, DEVELOPMENT & ENGINEERING

OWENS-ILLINOIS

GENERAL OFFICES TOLEDO 1 OHIO

SPONSORED BY

ADVANCED RESEARCH PROJECTS AGENCY

ARPA ORDER NO. 1441

PROGRAM CODE P9D10

FINAL TECHNICAL REPORT

By: N. L. Boling, M. D. Crisp, G. Dube,
L. Spanoudis, and P. R. Wengert

DAMAGE THRESHOLD STUDIES OF GLASS LASER MATERIALS

30 June 1972

CONTRACT NO. DAHC15-69-C-0303

Details of illustrations in
this document may be better
studied on microfiche

CONSUMER & TECHNICAL PRODUCTS GROUP

OWENS-ILLINOIS, INC.

TOLEDO, OHIO

PHONE: (419) 242-6543, EXTENSION 33-003

FOREWORD

This report has been prepared by the Consumer & Technical Products Group of Owens-Illinois, Inc., Toledo, Ohio under Contract DAHC 15-69-C-0303.

Dr. Norman L. Boling was the Principal Investigator. Dr. George Dube and Dr. Michael Crisp, scientists, Mr. Ted Phillips and Mr. David Wahl, technicians, assisted in the damage studies.

Dr. Paul R. Wengert was responsible for the thermodynamic studies. He was assisted by Mr. Louis Spanoudis and Mr. Paul Train, engineers.

Drs. Crisp and Wengert are in the Corporate Research Laboratory of Owens-Illinois.

A portion of the thermodynamics study (an empirical determination of activities) was subcontracted to the Battelle Memorial Institute, Columbus, Ohio. Dr. C. A. Alexander was responsible for that study.

The views and conclusions contained in this document are those of the authors, and should not be interpreted as necessarily representing the official policies, either expressed or implied, of the Advanced Research Projects Agency, or the U.S. Government.

This report is unclassified.

ABSTRACT

A summary of recent investigations of surface damage of transparent dielectrics is presented. For 30 nsec pulses at normal incidence, exit surface damage thresholds are typically 100 j/cm^2 for ED-2 laser glass. Asymmetry between the entrance and exit surface damage thresholds is explained by considering electric field strengths at the surfaces. The morphology of surface damage is described and a model based upon reflections from the laser induced plasma is proposed.

The problem of Platinum inclusions is not completely solved. Careful attention to the melting procedure has produced glass capable of withstanding energy densities much higher than the 10-20 j/cm^2 (30 nsec) limit of several years ago. Continuation of this approach holds promise of completely eliminating Platinum inclusions from laser glass.

TABLE OF CONTENTS

LIST OF FIGURES

LIST OF TABLES

I. INTRODUCTION AND SUMMARY

This is the final report on Contract DAHC 15-69-C-0303. Work on this contract began 1 July, 1969, and has covered several aspects of laser induced damage to glass. Damage due to platinum inclusions and surface damage have been studied extensively. Self tracking damage has been investigated, but to a lesser extent. Details of these studies can be found in previous semi-annual reports and no attempt will be made here to recapitulate results covered in those reports, except for a brief review of work on platinum inclusions in Part III. The emphasis in this report will be on work accomplished during the six months since the last semi-annual report. This work has been devoted to surface damage and the thermodynamics of melting laser glass in platinum crucibles.

Much has been learned about platinum inclusions during this contract. Although the problem has not been completely solved, laser glass melted in platinum and capable of withstanding energy densities much higher than the 10-20 J/cm^2 (30 ns) limit of several years ago is now commercially available. This has largely come about because of extreme care in the melting procedure. Continuation of this approach in conjunction with the results of the thermodynamic study conducted under this contract holds promise of completely eliminating damaging platinum inclusions from laser glass.

In the investigation of surface damage, a well controlled single transverse mode laser has been constructed. This laser emits several joules and allows use of a relatively large beam to study damage. Careful measurements made with this system have shown that the surface damage threshold of ED-2 laser glass is at least 80-120 J/cm^2 (30 ns, exit surface). This threshold is much greater than it was believed to be as recently as 1971.

The reason for the well known asymmetry in entrance and exit damage thresholds has been found to be Fresnel reflections at the air-dielectric interfaces.[1] This explanation emphasizes the importance of the local electric field in damage, and it will have an impact on the study of laser damage to dielectric surfaces in general. Already an extension of the theory shows that elimination of microscopic scratches and digs should greatly increase the threshold in some dielectrics.[2] Indeed, this has been experimentally demonstrated in the case of ion polished sapphire.[3] This theory will also serve as a guide to other treatments that might enhance the surface damage threshold of laser glass.

Another asymmetry investigated is the morphological difference in damage at entrance and exit surfaces.[4] Circumstantial evidence strongly indicates that reflection of the laser pulse from the plasma associated with damage in many dielectrics is responsible for the difference in damage form.

From the work in this and other laboratories, the physics of surface damage is beginning to be understood. Although much remains to be done, the prospects for greatly increased surface damage thresholds in glass are good.

II. DAMAGE STUDIES

II-1. DEFINITION OF DAMAGE

In order to discuss laser induced surface damage of transparent dielectrics, one must clearly define damage. It is generally agreed that a change, which can be microscopic, in the appearance of the surface constitutes damage. A point of greater contention is whether a visible plasma always accompanies such a change. If it could be established that the occurrence of a visible plasma is a necessary and sufficient condition for surface degradation, then the plasma could logically be used as a definition of damage. This relationship does not, however, hold for all transparent dielectrics. In damage testing a high index of refraction glass with a very low surface damage threshold, we have consistently observed relatively gross damage without a plasma. Plasma formation in this glass did not occur until energy levels approximately four times the damage threshold were reached. In the studies reported here, Owens-Illinois ED-2 laser glass samples polished to commercial specifications were investigated. Experimental results for this glass are discussed for two geometries: in one the laser beam strikes the surface at near normal incidence and in the other at Brewster's angle. In other geometries or materials damage can occur without an accompanying plasma; but in the two geometries specified above damage was never detected without plasma, and vice versa. Therefore, for the experimental results reported herein, the damage threshold of a surface is defined as the lowest energy density which produces a visible plasma.

II-2. EXPERIMENTAL ARRANGEMENT AND PROCEDURE

The single transverse mode laser used in this study consists of an oscillator and four amplifiers. The characteristics of the oscillator have been reported earlier[8] and will not be repeated here. The first three amplifiers use Brewstered 3/4 inch diameter by 13 inch length rods. Each rod is water cooled and pumped by two helical flashlamps. The fourth amplifier is similar but is only 7 inches long and is pumped by one helical flashlamp.

A three millimeter aperture is used in the oscillator to achieve single mode operation. By expanding the resulting three millimeter beam, through the use of lenses placed in the amplifier chain, 35 joules in 30 nanoseconds has been obtained from the system. When an optical shutter is used to obtain 2 ns pulses, this degree of amplification is required to achieve sufficient energy fo large beam testing. Although a shutter has been installed and checked out in the system, it has not been used in the studies reported here. In these studies no beam expanding optics have been used and the amplifiers are pumped at low levels. The result is a high quality beam of several joules in 30 ns. This energy is more than sufficient to yield a beam of almost 2mm on the sample to be tested.

Characteristics of the laser output are given in Table 1. Figure 1 shows the arrangement used to measure the energy density on the sample. In order to minimize any self-focusing effects, the sample position was chosen to be at the waist of the focused laser beam. A specially designed 1mm aperture was placed at the position to be occupied by the sample. This aperture was moved across the beam until maximum energy passed through it, the laser being pumped at the same level on every shot. To insure that no energy in the pulse was absorbed by a plasma forming in the aperture, calibrated filters

TABLE 1. LASER CHARACTERISTICS

Transverse Mode	TEM_{oo}
Longitudinal Modes	Many (No Control)
Pulse Width	30 ns FWHM
Polarization	Linear
Time Interval Between Pulses	7-10 min
Energy Output	5-12 joules
Reproducibility of Energy Output	± 10%
Beam Diameter at Position of Glass Sample (Exit and Entrance Surfaces)	1.8 mm

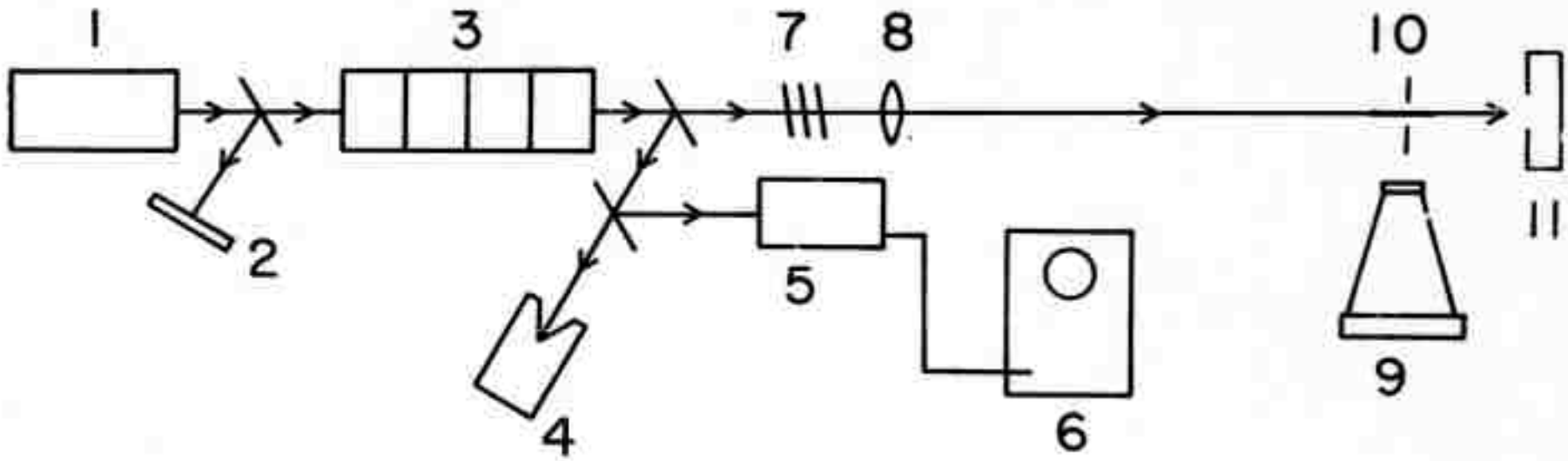

Figure 1 - Apparatus used for energy density measurements. The components are: (1) neodymium glass laser oscillator; (2) Polaroid film; (3) neodymium glass laser amplifier chain; (4) thermopile; (5) photodiode; (6) Tektronix 519 oscilloscope; (7) neutral density filters; (8) 1.5 m focal length lens; (9) camera; (10) aperture; (11) thermopile.

were added in the path of the beam until photographs of the aperture taken with an open shuttered camera during the laser pulse showed no plasma. Further verification of the absence of a plasma was obtained by changing the transmission of the filters by a given factor and noting that the energy passing through the aperture changed by the same factor. Prior to this the filters were checked for bleaching during the laser pulse and no such bleaching was observed.

Several thermopiles were checked for use in these measurements and readings among these varied by ± 10%. Even recent calibration did not insure readings more consistent than this. Aside from the thermopile used, the nature of any other error in this calibration, such as positioning of the aperture off beam center, would have resulted in an underestimation of the average energy density over the aperture. Based upon the assumed Guassian cross section of the beam, the peak energy density was calculated to be 25% higher than the average taken over the 1mm aperture.

The arrangement of Figure 1 was also used to monitor and control energy on the samples during damage tests, the only difference being that the aperture and thermopile were replaced by the sample. The pulse width, transverse mode, and energy out of the laser were monitored on all shots. The laser was always pumped at the same level, the energy on the sample being controlled by changing filters. Because the transmission of the filters was changed in steps of 10% and the reproducibility of the laser output was ± 10%, the thresholds measured are relatively accurate to within 20%.

The samples used for testing were never more than 1/2 inch thick. This length, in conjunction with the 1.5 m focal length lens used to focus the beam onto the sample, insured that the beam was the same diameter at the entrance and exit faces.

Several cleansing procedures were tried before settling on one which seemed to give satisfactory results. This final procedure consisted of ultrasonic cleaning in a soap and water solution, a rinse in distilled water, and cleaning in the vapors of boiling isopropyl alcohol, in that order. Final examination for cleanliness consisted of careful visual examination under a bright microscope light. Great care in cleaning had to be exercised before a sample would pass this inspection. Damage tests were begun immediately after cleaning of the sample. For a given sample these tests typically required a minimum of two hours. Thus the condition of the sample was representative of surfaces in a carefully cleaned laser system.

II-3. MEASURED DAMAGE THRESHOLDS

Damage thresholds will be reported here in terms of the average energy density measured over the 1mm aperture used for system calibration. When the calculated higher peak density and nature of any errors in the calibration technique are taken into account, these thresholds are seen to be conservative. That is, the thresholds are at least as great as reported here. Nevertheless, the exit threshold for ED-2 typically varied between 80 and 120 J/cm^2 (2.7 - 4 GW/cm^2) and the entrance threshold between 120 and 200 J/cm^2 (4 - 6.7 GW/cm^2). This is significantly higher than the 40-50 J/cm^2 threshold previously thought to apply to most laser glass, but it is in good agreement with previous measurements made on the same glass with a large beam multimode laser . In making comparisons with thresholds of dielectrics reported elsewhere, it should be carefully noted whether these thresholds were measured on the entrance or exit surface. This point is sometimes not made clear. A theory for calculating the exit threshold from a given entrance threshold, or vice versa, will be given in Section II-5 of this report.

The wide spreads in thresholds reported here are typical of damage measurements in transparent dielectrics. There are two plausible reasons for this. First, the process which triggers the damage might be inherently probabilistic[7]. In connection with this it should be remembered that the beam diameter of the experiments discussed here is much larger than that used in the experiments described in Reference 7. The probability of damage on any given shot is a function of the size of the damaging beam, as has been pointed out by the author (Reference 7). The second reason for the spread lies in the condition of the surface. Visible scratches on the surface can greatly lower the damage threshold. Furthermore, there is very good reason to believe that even microscopic defects in the surface can lead to damage[4].

II-4. SURFACE STRENGTHENING AS A MEANS OF INCREASING THE DAMAGE THRESHOLD

Since some theories of surface damage involve mechanical breakage, a strengthening of the surface presents itself as a possible method of increasing resistance to damage. We have used an ion exchange process on ED-2 glass to examine this approach. In this process lithium atoms in the surface are replaced by sodium atoms. This results in a "crowding" of atoms on the surface, leading to a surface compression layer. The layer was about 200 microns deep in the work described here. Glass so treated exhibits greatly increased mechanical strength.

No measurable increase in the damage threshold was noted for these ion exchanged samples. However, the morphology of the damage was quite different from that seen on untreated glass. Damage near threshold was much like that described in Section II-6 of this report for untreated samples. In particular, the ring structure was present immediately after the damaging shot. Within

a few minutes after the shot no damage could be seen inside the ring, except for a slight rippling of the surface. However, over a period of time ranging up to two days the surface inside the ring often gradually developed a tessellated pattern. Figures 2 and 3 show respectively exit damage a few minutes and one day after the damaging shot. Out of fifteen damage sites examined on ion exchanged samples, eight exhibited this cracking phenomenon. The same thing is sometimes seen on the entrance faces of untreated samples, but much less often and only after exposure to very high power levels.

It is of interest to note that cracking of the ion exchanged surfaces is due to the hot plasma and not the laser pulse. Just as on untreated surfaces, these cracks often fill the interior of the several millimeter diameter ring, but they never extend outside the ring.

A possible reason why ion exchanged glass exhibits delayed failure to a greater extent than untreated glass is that the thermal expansion coefficient of glass is a strong function of the quality and quantity of its alkali content. A sodium glass has a greater expansion coefficient than the same glass with lithium. Thus plasma heating of the sodium rich surface of an ion exchanged sample may result in much greater stresses than in the case of an untreated lithium containing surface.

Still another and perhaps more plausible reason for the delayed failure is the difference between stress in the surface layer and stress in glass immediately below the surface. This stress difference could be greatly increased through heating by the plasma and subsequent rapid cooling of the surface layer.

Figure 2 - Exit damage on mechanically strengthened cube a few minutes after damaging shot.

Figure 3 - Exit damage of mechanically strengthened cube one day after damaging shot.

At the time these experiments on strengthened surfaces were conducted, the theory of Sections II-5 and II-6 of this report had not yet been developed. With this theory and its extension to surface defects, it might have been predicted that mechanical strengthening would not be efficacious in raising the threshold. Hopefully, many other possible treatments of surfaces can be eliminated on the basis of this increased theoretical knowledge.

II-5. IMPORTANCE OF REFLECTIONS IN SURFACE DAMAGE

One of the more puzzling aspects of laser surface damage experiments has been the observed asymmetry in damage thresholds of the entrance and exit surfaces of a sample. It is observed[8] that when a high-power laser pulse passes at normal incidence through a transparent dielectric material such as glass, the threshold for optical damage of the exit surface is less than the threshold for damage of the entrance surface. Attempts have been made to explain this asymmetry in terms of the propagation of acoustical phonons which are generated by the light[8] and in terms of an asymmetry in the direction of growth of the plasma which always seems to accompany surface damage.[9] However, neither these nor other proposed mechanisms have been able to quantitatively explain the experimental observations. One source of asymmetry which is present in these damage experiments is the Fresnel reflections from the entrance and exit surfaces. It was shown in Reference 1 that reflections can be quite important in determining surface damage thresholds.

Consider a light pulse that enters an isotropic optical material at near normal incidence, as shown in Figure 4; there will be a reflection at the air to sample boundary. Since the index of refraction n of material is greater than that of air, the reflection light wave E_{R1} suffers a phase shift of

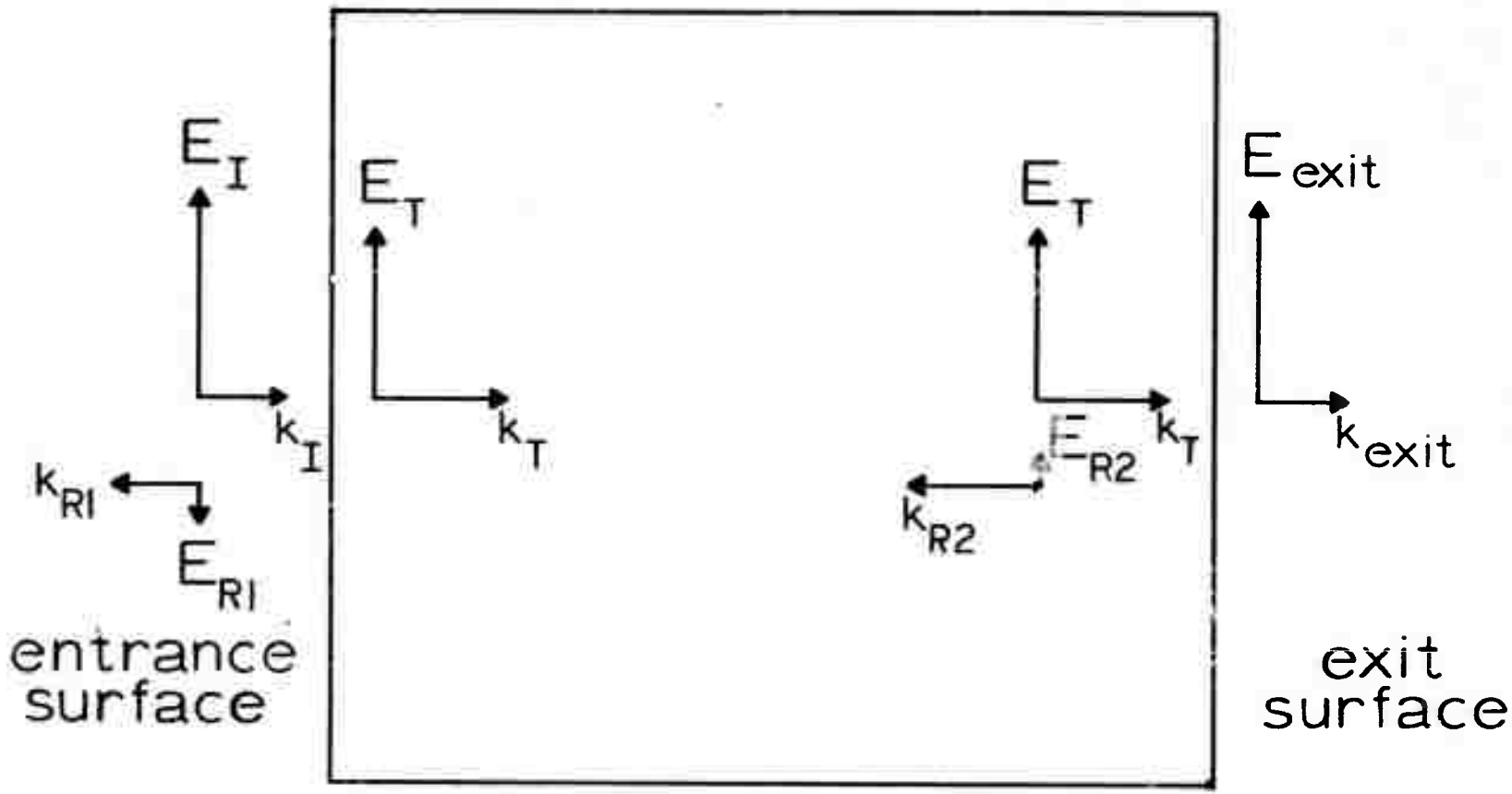

Figure 4 - Electric fields at the entrance and exit faces of a dielectric sample. The light is incident from the left at near normal incidence. The wave vectors of the light incident on and reflected from the entrance face are $\vec{k}_I$ and $\vec{k}_{RI}$, respectively. The wave vectors of the light that is incident on, reflected from and transmitted through the exit faces are $\vec{k}_T$, $\vec{k}_{R2}$, and $\vec{k}_{exit}$, respectively.

180° with respect to the incident light wave. This phase shift results in a partially destructive interference of the two light waves within a distance of $\lambda/4$ outside the entrance surface. Boundary conditions require that the electric vector be continuous across the surface so the effect of interference between the incident and reflected light reduces the amplitude of the oscillating electric vector experienced throughout the vicinity of the entrance surface. The reduction of the electric field strength at the entrance surface is a surprisingly large effect. Application of Fresnel's equations [10] shows that the amplitude of the oscillating electric vector in the vicinity of the entrance surface is given by

$$E_{ent.} = \frac{2}{n+1} E_I \qquad (1)$$

where E_I is the amplitude of the electric vector that comes out of the laser. For a glass of index of refraction n = 1.5 this corresponds to a reduction of the electric field at the entrance surface to 4/5 of the electric field of the laser pulse.

The light pulse that is transmitted through the sample suffers a second reflection at the exit surface. This time the pulse is passing from the sample to the air and there is no phase shift of the reflected light beam. Interference between the light incident on and reflected from the exit surface results in an increase of the electric field vector at the boundary to a value [10]

$$E_{exit} = \frac{4n}{(n+1)^2} E_I \qquad (2)$$

which is 0.96 times the incident electric field for a glass of index of refraction n = 1.5. The lack of a phase shift during reflection at the

sample-air interface gives rise to an electric field maximum at the boundary. Additional maxima occur at integral multiples of one-half a wavelength from the exit face for a distance of approximately a coherence length. Higher order effects would occur if the front of the light pulse reflected from the exit surface propagated back to the entrance face and overlapped a latter portion of the entering pulse. Such effects constitute an unnecessary complication to the analysis of the experiment and are eliminated when the incident light beam makes a small angle with the surface normal.

Equations (1) and (2) give the electric field amplitudes experienced by the entrance and exit surfaces when a light pulse of amplitude E_I is incident on a sample at near normal incidence. In order to make predictions concerning damage thresholds for such expressions it is necessary to make specific assumptions about the damage mechanism. To treat the normal incidence experiments it is sufficient to assume that the probability that a surface damages is a function of the amplitude of the oscillating electric field in the vicinity of the surface. This assumption would not be sufficient to describe the threshold asymmetry if stimulated Brillouin scattering or self-focusing in the bulk material were responsible for surface damage. A definite prediction of the ratio of entrance to exit damage thresholds follows from this very general assumption.

If the dielectric surface damages when it is exposed to an oscillating electric field of amplitude E^D then from Equation (1) the amplitude of the incident laser pulse would have to be equal to

$$E^D_{ent.} = \frac{(n+1)}{2} E^D \qquad (3)$$

in order to damage the entrance face. Similarly from Equation (2) it follows that for exit damage the amplitude of the incident laser pulse would have to equal

$$E^D_{exit} = \frac{(n+1)^2}{4n} E^D \quad . \tag{4}$$

In an experiment one measures the power per unit area S^D (averaged over many optical cycles) of the damaging pulse, which is proportional to the square of the electric field. By taking the ratio of the square of Equation (3) to the square of Equation (4) it is predicted that the ratio of the power per unit area required to damage the entrance surface $S^D_{ent.}$ to the power per unit area required to damage the exit surface S^D_{exit} is

$$\frac{S^D_{ent.}}{S^D_{exit}} = \frac{4n^2}{(n+1)^2} \quad . \tag{5}$$

If Fresnel reflections are the only contributors to the asymmetry in damage thresholds Equation (5) implies that the ratio of the entrance to the exit threshold is a function only of the index of refraction of the dielectric. This ratio equals 1.48 for Owens-Illinois ED-2 glass which has an index of refraction n= 1.55. A series of measurements of the entrance and exit damage thresholds of ED-2 glass was made and the average value of the ratio was found to be 1.6 ± 0.4. This indicates that the magnitude of the asymmetry which is predicted on the basis of Fresnel reflections is large enough to explain the experimental observations.

A further confirmation of the importance of Fresnel reflections to surface damage thresholds was obtained by making measurements with a Brewster's angle geometry. A light pulse that is polarized in the plane of incidence will

experience no reflection when incident on a sample at Brewster's angle. If Fresnel reflections were the only contributor to the observed asymmetry in damage thresholds then one would expect both surfaces of a sample to exhibit the same damage threshold when the experiment is carried out at Brewster's angle. To investigate this prediction, measurements of entrance and exit damage thresholds were made with a beam incident at Brewster's angle on disks of 2mm thickness ED-2.3 laser glass (3 weight percent Nd doping). It was found that the two surfaces of the samples usually damaged at the same energy density.

Interference between incident and reflected light waves will in general be important for experiments done at oblique angles of incidence other than at Brewster's angle. Lyubimov, Fersman and Khazov[11] have investigated the thresholds for surface damage for a light wave that undergoes total internal reflection within a prism. The analysis of their experiment which is presented in Reference 11 erroneously ignored the fact that there is a phase shift upon total internal reflection which is a function of the angle of incidence. The authors of Reference 11 also did not take into account the reduction of the electric field at the entrance face of the prism due to the interference effects described above.

A correct analysis of an experiment involving a total internal reflecting (TIR) surface will be presented below and it will be seen that a careful measurement of the damage thresholds for this experiment can provide information concerning the functional dependence of the damage mechanism. The treatment presented here is an extension of the analysis of Reference 12.

Consider an experiment in which a light wave undergoes two internal reflections in a Porro prism (see Figure 5). If the light wave incident upon

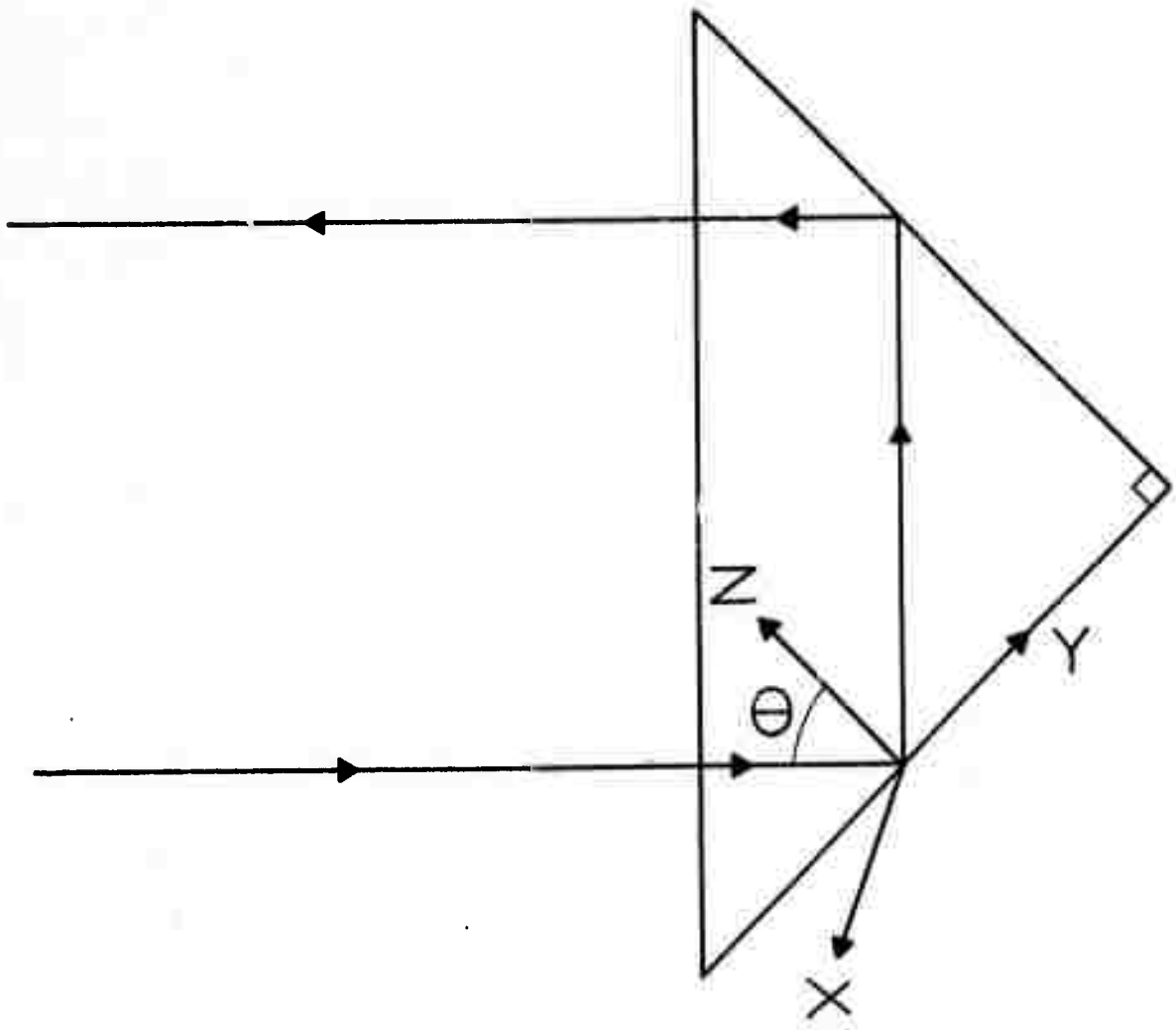

Figure 5 - Coordinate system used to analyze a surface damage experiment involving total internal reflection.

the prism is polarized in the plane of the figure (p polarization) then its electric field can be written

$$\vec{E}_I = E_0(\hat{e}_z \sin\theta + \hat{e}_y \cos\theta) \cos\omega[t - (y \sin\theta - z \cos\theta)/c] \quad . \qquad (6)$$

It was shown above that interference between incident and reflected waves at the entrance surface reduces the light field at the entrance face to a value

$$\vec{E}_{ent.} = \frac{2}{n+1} \vec{E}_I \quad . \qquad (7)$$

Hence the electric field of the light that is incident on the first TIR surface is

$$\vec{E}_T = \frac{2}{n+1} E_0(\hat{e}_z \sin\theta + \hat{e}_y \cos\theta)\cos\omega[t - (y \sin\theta - z \cos\theta)n/c] \quad . \qquad (8)$$

The reflected light wave has the form

$$\vec{E}_R = \frac{2}{n+1} E_0(\hat{e}_z \sin\theta - \hat{e}_y \cos\theta)\cos[\omega t - (y \sin\theta + z \cos\theta)\omega n/c + \delta_p] \qquad (9)$$

where the phase shift δ_p is given by[10]

$$\tan(\delta_p/2) = -\sqrt{n^2\sin^2\theta - 1} \,/\, \cos\theta \quad . \qquad (10)$$

The electric field experienced at the first TIR surface (which is defined by z=0 in Figure 5) is due to the superposition of the fields of Equation (8) and Equation (9).

$$\vec{E} = \frac{4}{n+1} E_0\left[\hat{e}_z \sin\theta \cos\left(\omega t - \frac{n\omega}{c} y \sin\theta + \frac{\delta_p}{2}\right)\cos(\delta_p/2)\right.$$
$$\left. + \hat{e}_y \cos\theta \sin\left(\omega t - \frac{n\omega}{c} y \sin\theta + \frac{\delta_p}{2}\right)\sin(\delta_p/2)\right] \quad . \qquad (11)$$

This calculation can be repeated for light polarized perpendicular to the plane of the diagram (s polarization). In this case the light wave incident on the first TIR surface will have the form

$$\vec{E}_T = \frac{2}{n+1} E_0 \hat{e}_x \cos \omega[t-(y \sin \theta - z \cos \theta)n/c] \qquad (12)$$

and the light wave reflected from the surface will be given by

$$\vec{E}_R = \frac{2}{n+1} E_0 \hat{e}_x \cos[\omega t-(y \sin \theta + z \cos \theta)\omega n/c + \delta_s] \qquad (13)$$

where the phase shift is given by[6]

$$\tan (\delta_s/2) = - \sqrt{n^2 \sin^2 \theta - 1} \,/\, n \cos \theta \quad . \qquad (14)$$

The resultant electric field at the surface is

$$\vec{E} = \frac{4}{n+1} E_0 \hat{c}_x \cos(\omega t - y \sin \theta n\omega/c + \delta_s/2)\cos(\delta_s/2) \quad . \qquad (15)$$

The tip of the electric field vector described by Equation (11) tranverses an elliptical path in the yz plane. The electric vector of Equation (15) executes a simple harmonic oscillation along the x-axis. Before conclusions can be drawn from Equations (11) and (15) concerning damage thresholds, an additional assumption has to be made about the damage mechanism. Earlier it was assumed that the probability that a surface would damage is a function of the amplitude of the oscillating electric field at the surface. This single assumption was sufficient to explain the observations for the normal incidence geometry because all the electric vectors executed harmonic motion along an axis in the plane of the surface. The TIR geometry allows the possibility of different directions of the electric vector with respect to the surface normal and a time dependence that is not simply harmonic.

Two hypotheses will be investigated here. If the damage mechanism were simply the analog of a dc breakdown due to the high electric fields of the light wave then it would be reasonable to assume that the probability of damage depends on (i.e., is a function of) the maximum electric field strength that occurs in Equation (11) or Equation (15). On the other hand, if the probability of damage depends on the average energy density present at the surface then the damage threshold should be proportional to the time average of the square of Equation (11) or Equation (15). Neither of these hypotheses takes into account that the damage threshold may depend on the directions of the electric vector with respect to the surface and not just its magnitude.

If a surface damages when it experiences an oscillating electric field of maximum amplitude greater than or equal to E^D then Equation (7) implies that the entrance surface would damage when the incident light amplitude is equal to

$$E^D_{ent.} = (n+1)\, E^D/2 \tag{16}$$

and the first TIR surface would damage when the light wave incident on the entrance face has an amplitude

$$E^D_p = \frac{(n+1)\sqrt{n^2-1}}{2\sqrt{2}}\, E^D \tag{17}$$

and

$$E^D_s = \frac{(n+1)\sqrt{n^2-1}}{2\sqrt{2}\, n}\, E^D \tag{18}$$

for the p and s polarizations, respectively. The angle of incidence θ has been set equal to 45° in order to compare with the experimental results reported in Reference 11.

Regardless of the particular functional dependence of the damage threshold upon the electric field at the surface, experiments measure the power per unit area of the damage pulse which is proportional to the average of the square of the electric field vector. Equations (16), (17) and (18) imply that the ratio of damage thresholds for the entrance and first TIR surfaces for the p and s polarizations would be

$$1:[(n^2-1)/2]:[(n^2-1)/2n^2] \quad , \tag{19}$$

respectively. The experimental measurements of Reference 11 were reported for K-8 glass of index of refraction n = 1.5. When this value is substituted into the expression above the predicted ratio of damage thresholds is 1:(1/1.6):(1/3.6). This is in good agreement with the experimentally observed ratio of 1:(1/1.64):(1/3.85) reported in Reference 11.

If, on the other hand, one assumed that the probability that a surface would damage depended on the average energy density at the surface then a surface would damage when it was exposed to an energy density (averaged over an optical period) which was greater than or equal to U^D. For this dependence of damage threshold one would predict from Equations (7), (11) and (15) that the entrance surface would damage when the energy density of the incident light wave was

$$U^D_{ent.} = (n+1)^2 U^D/4 \tag{20}$$

and the TIR surface would damage when the energy density of the incident pulse was

$$U^D_p = \frac{(n+1)^2}{8} U^D \tag{21}$$

and

$$U^D_s = \frac{(n+1)^2(n^2-1)}{8n^2} U^D \tag{22}$$

for polarizations in and normal to the plane of incidence, respectively.

Equations (20), (21) and (22) lead to a prediction of a ratio of damage thresholds which is

$$1:(1/2):[(n^2-1)/2n^2] \quad . \tag{23}$$

For a dielectric of index of refraction n = 1.5 the predicted ratio is 1:(1/2):(1/3.6). Thus the two hypotheses differ in the prediction of the ratio of the threshold for the p polarization to the other thresholds and the assumption that the probability of damage depends on the maximum electric field is in better agreement with the experimental damage thresholds reported in Reference 11. The accuracy of the measurement reported in Reference 11 is not stated so it is not clear whether the agreement is significant.

If the probability that a surface would damage depended on the maximum electric field experienced at a surface and not on the average energy density then one would expect damage thresholds measured at normal incidence with elliptically polarized light to be higher than those measured with linearly polarized light. A circularly polarized light wave of maximum amplitude E_0 can be written

$$\vec{E}_c = E_0[\hat{e}_x \cos(\omega t-kz) + \hat{e}_y \sin(\omega t-kz)] \quad . \tag{24}$$

This light wave contains an average energy density

$$U_c = \frac{E_0^2}{4\pi} \quad . \tag{25}$$

A linearly polarized light wave having a maximum ampitude E_0 can be written as

$$\vec{E}_L = E_0 \hat{e}_x \cos(\omega t-kz) \tag{26}$$

and would have an average energy density of

$$U_L = \frac{E_0^2}{8\pi} \tag{27}$$

which is one-half the average energy density of the circularly polarized light. The signal of a fast photodetector is proportional to the average energy density of the light pulse. One is thus led to the conclusion that if the probability of damage depends on the maximum value of the electric field vector and not the average of its square then the damage threshold for circularly polarized light will be twice that of linearly polarized light. A preliminary comparison of surface damage thresholds for circularly and linearly polarized light has been carried out and no significant difference in thresholds was found. This result has motivated us to try and duplicate the TIR measurements of Reference 11. That experiment is in progress.

The ideas of Reference 1 concerning the importance of the electric field strengths at the surfaces of a dielectric have recently been extended by Bloembergen[7] to investigate the role of submicroscopic cracks and pores in surface damage. It is found that these surface characteristics can act to concentrate the electric field strength to values comparable to those that have been observed to produce damage in the bulk material.

In summary, it has been fairly well established that the value of the electric field vector in the vicinity of the surface of a material is important for determining whether the material will exhibit surface damage. Thus care should be taken in designing damage resistant optical components so that interference effects that lead to maximum electric field strengths located at the surface of a material are avoided. If possible, interference should result in minimum values of the electric field strength at the surfaces. For example, it was seen that a minimum electric field strength would naturally occur at the entrance surface of a sample. Similar considerations should be taken about the standing waves that occur in dielectric

coatings. Furthermore it was seen that the measurement of damage thresholds for different geometries and polarizations can provide information concerning the functional dependence of the damage threshold upon the electric vector at the surface.

II-6. MORPHOLOGY OF DAMAGE

It was seen in the last section that the asymmetry between exit and entrance damage thresholds is adequately explained by considering the electric field amplitudes that result in the vicinity of the surface when reflections are taken into account. However, the discussion did not explain the difference in the qualitative character of entrance and exit damage. At energy densities sufficiently above threshold, exit damage typically takes the form of a pit, while entrance damage consists of a crazing or cracking of the surface with little removal of material. Near the threshold for either surface there is no qualitative difference between entrance and exit damage for ED-2 laser glass.

Figure 6 shows damage that is typical of either the entrance or exit surface for energy densities near threshold. The ring structure seen in the photo consists of material deposited on the surface. This deposit cannot be removed by hard rubbing with acetone or isopropyl alcohol. The form of the structure varies; sometimes it consists of a single ring and sometimes it consists of several concentric rings. The diameter of these rings can range from approximately the diameter of the damaging beam to several times this size. In Figure 6 the ring structure is 4mm across while the beam was 1.8mm. Generally, the diameter of the ring increases with the energy of the beam. Although the effect is not easily discernible in micrographs, the surface inside the rings always exhibits a rippling or "orange peel" appearance.

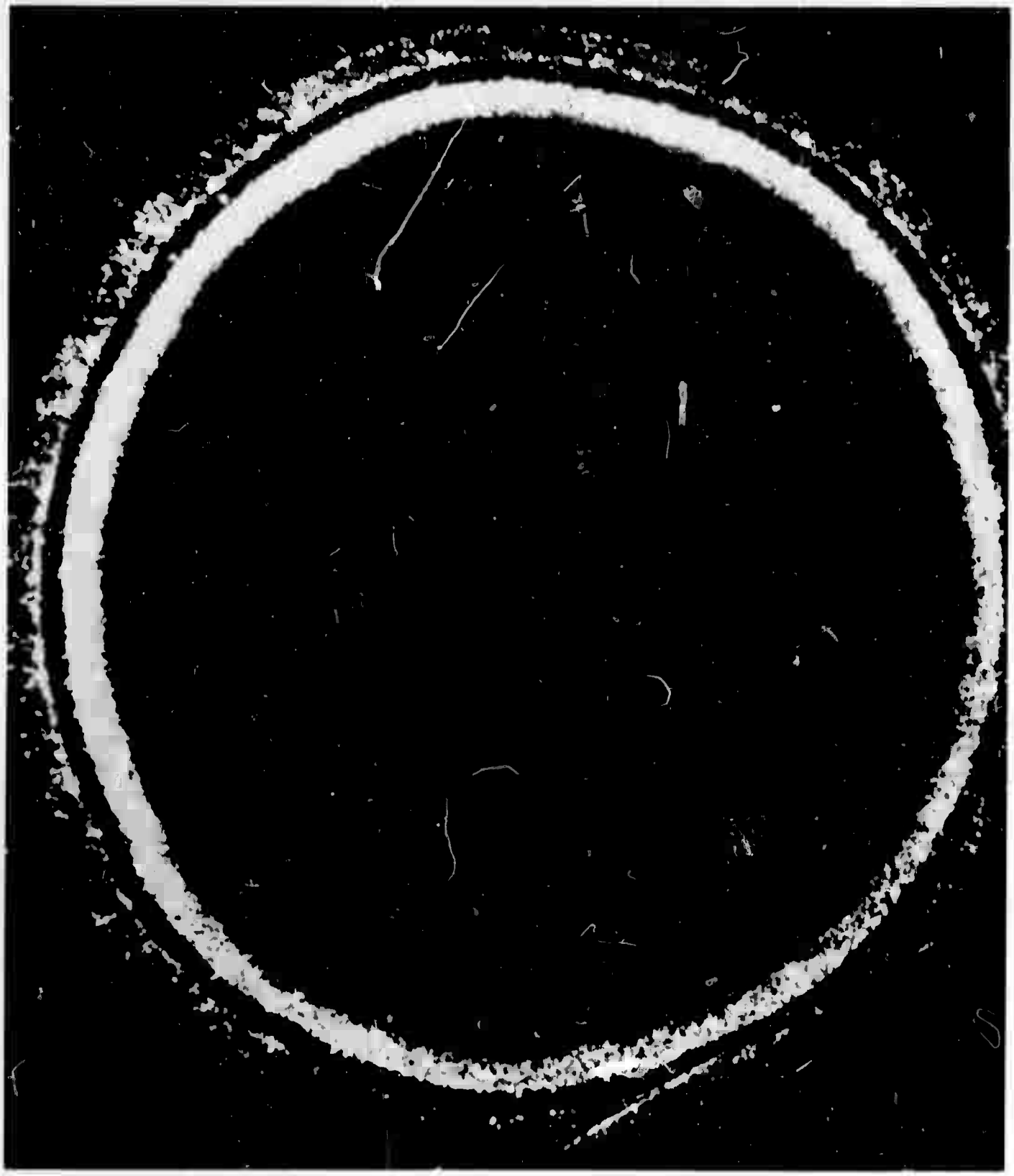

Figure 6 - The ring structure shown in this figure is typical of damage for either the entrance or exit surface when the incident pulse is near threshold.

Occasionally, some cracking of the surface is seen inside the ring at this stage. Since the rings can be much larger than the damaging beam, it can be concluded that they are caused by the plasma and not the beam. This conclusion is supported by the absence of rings on a glass in which damage occurs without an accompanying plasma.

A possible explanation of ring formation is as follows. The initial plasma is formed in the region of the damaging beam. Its temperature is greater than 10^4 °K as it begins to expand over the surface.[21] The hot plasma heats the surface where it comes into contact with it. It is this heating that causes the ripple effect seen at both surfaces at this stage of damage. The plasma is cooled by expansion and by contact with the cooler surface. As the plasma cools, different components condense out at different temperatures, forming the system of rings. This explanation is consistent with the observation that cracking or rippling of the surface never extends beyond the ring but sometimes fills the entire ring. Confinement of damage to the interior of the ring indicates that the plasma is significantly hotter inside the ring than outside. Furthermore, on the basis of this explanation it might be expected that the most volatile component of the glass would be evaporated by the plasma first and the ring structure, when there is a single ring, would consist primarily of this component. In the case of ED-2 the most volatile component is Li_2O. The composition of a single ring was analyzed with an Auger spectrometer and it was found that the ring was rich in lithium compared to the surrounding unchanged glass. This observation is consistent with the results reported in Reference 13. A multiple ring structure has not yet been analyzed.

Figures 7 and 8, respectively, show typical entrance and exit damage at energy densities well above the damage threshold. Energy densities in excess of 1.4 times the threshold are sufficient to cause pitting of the exit surface. Pitting becomes more severe as the energy density is increased. The cracking seen at the entrance surface never extends beyond the ring structure associated with the shot causing the damage, but the network of cracks sometimes grows and continues to fill in the ring several hours after the damage is perpetrated. This behavior is seen often on surfaces which have been mechanically strengthened by inducing a high compressional stress in the surface through an ion exchange process.

Several models have been presented in attempts to account for the asymmetry in damage morphology at the two surfaces. It has been proposed[9] that the shock resulting from growth of the plasma into the laser beam, and consequently into the exit surface, causes exit pitting. However, streak photos of the entrance and exit plasmas have shown that the plasma grows away from the surface at both the entrance and exit.[3] This indicates, as pointed out in Reference 9, that asymmetric plasma growth is not an explanation for the observed difference in damage.

Stimulated Brillouin Scattering (SBS) has also been proposed as being responsible for exit pitting, as well as for surface damage in general.[8] Three arguments can be made that suggest SBS does not play a significant role in determining damage morphology. First, the analysis of Section II-5 shows that SBS is not necessary to explain the asymmetry in plasma formation threshold. Second, there is evidence that the SBS that occurs at powers used in damage studies is not intense enough to fracture glass surfaces.[14] Finally, even if the intensity were great enough, this mechanism should cause the

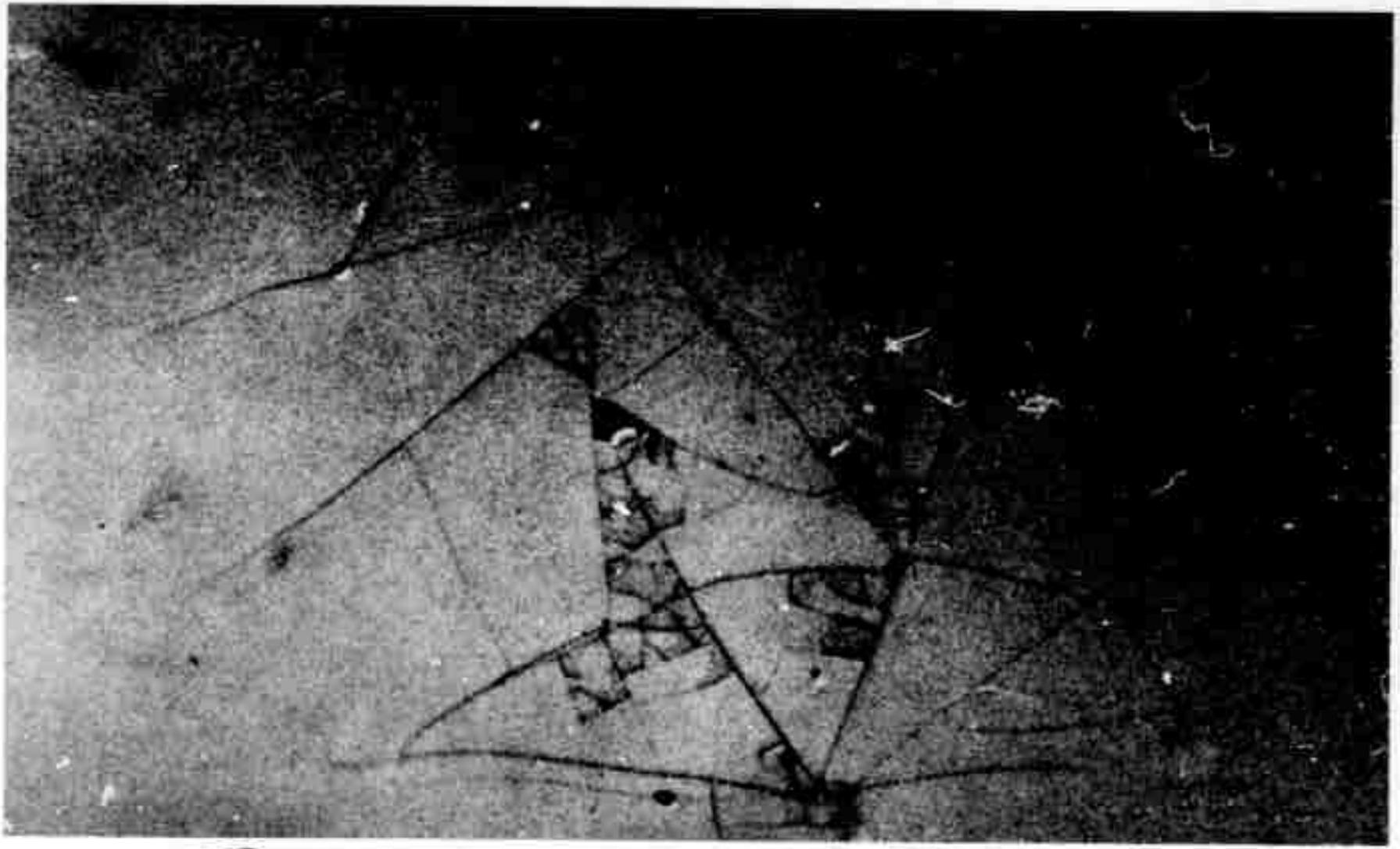

Figure 7 - Entrance damage when the incident energy density is well above threshold.

Figure 8 - Exit damage when the incident energy density is well above threshold.

most severe damage to occur at the entrance face where the acoustic wave is most intense. These three facts taken together provide strong evidence against using SBS as a significant factor in any explanation of damage morphology.

It has recently been proposed that in some cases electric surface stress can explain pit formation at the exit face.[15] In order to achieve the power densities required to induce an electric stress large enough to fracture glass, it was necessary to assume in Reference 15 that the damaging beam underwent self-focusing. However, in the experiments discussed herein no evidence of tracking damage was observed. Furthermore, the observation that the ratio of entrance to exit damage threshold can be explained without reference to self-focusing suggests that no self-focusing occurred in these experiments. The pitting damage reported here occurred at power densities of 5 GW/cm^2. Using the analysis of Reference 15 in the absence of self-focusing, this power density leads to an electric stress of approximately $1.5 \times 10^6 N/m^2$, far below the stress required for glass fracture. One might argue that the surface plasma formed during the first part of a damaging pulse weakens the glass surface through severe heating, and this weakened surface could then be pitted by electric stress. However, in the experiments described in this report electric stress does not seem to be an important factor in crater formation.

It has been argued above that none of the currently proposed models adequately explains the asymmetric morphologies described earlier. In the remainder of this section a new model will be presented in an attempt to account for the differences in morphology.[4] To this end the analysis of

Section II-5 will be extended to examine Fresnel reflections at the interface between the glass and the laser generated plasma that appears above threshold. That reflection from laser created plasmas can be significant, even in the absence of well defined surfaces, is well-known in controlled thermonuclear fusion work.[16]

At power densities above the damage threshold for a surface, plasma formation typically occurs before or near the peak of the damaging pulse.[17] The remainder of the pulse is therefore incident not upon a glass-air interface but upon a glass-plasma interface. Thus it is necessary to examine the electric fields that occur at or near this glass-plasma boundary if one is to understand how damage develops after plasma formation. In order to do this it is necessary to know something of the plasma characteristics.

A Q-switched ruby laser has been used at Owens-Illinois to take double exposure holograms of a one inch glass cube at various times after a pulse of power density well above the pitting threshold passed through it.[21] Figure 9 shows a schematic diagram of the experimental arrangement. A photo of the virtual image of one of these holograms is shown in Figure 10 the circular light in the background is from the ruby laser. The 30 ns damaging pulse from the Nd glass laser passed from left to right through the sample 1.4 μs before the hologram was taken. The exit plasma is clearly visible outside the sample, as are longitudinal and transverse acoustic waves propagating into the sample after having been produced at the surface crater during the damaging event. The opaque region in the center of the plasma is glass spalled from the crater. A series of such holograms taken at various times after the occurrence of damage can be used to study the time evolution of the plasma. The number of fringes in the plasma indicates

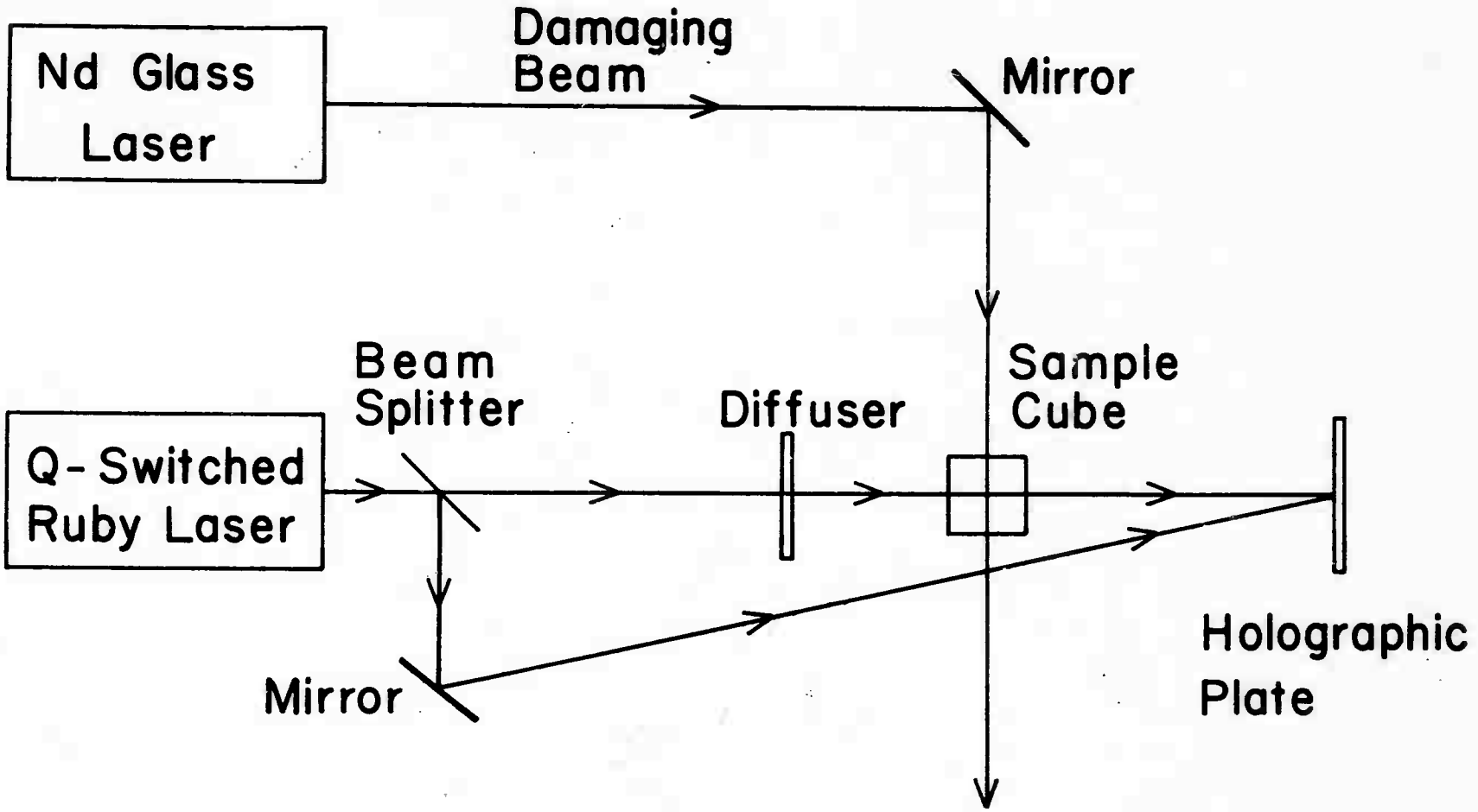

Figure 9 - Experimental arrangement used to make a hologram of the cube at a variable time after passage of the damaging pulse.

Figure 10 - Photograph of the virtual image of a hologram of a one-inch cube of ED-2 laser glass. The hologram was taken 1.4μs after a Q-switched-Nd-laser pulse passed through it from left to right causing a damage event.

an average free electron density. By measuring the size of the plasma at a given time and extrapolating to the estimated size of the initial plasma it can be shown that the free electron density is initially at least 10^{21} electrons/cm^3 when the energy of the damaging pulse is sufficiently above threshold. This calculation is supported by observations of transmission cutoff of a laser pulse passing through the plasma.[9] Through measurements of the plasma size at various times the plasma expansion velocity, and hence its temperature, can be estimated as a function of time. The plasma initially expands at 10^6 cm/sec in agreement with expansion velocities reported in Reference 3. This expansion velocity corresponds to a temperature of approximately 7×10^{4}°K. After 1.6μs the plasma has cooled to 4×10^{3}°K.

Holograms taken as early as 45 ns after the peak of the damaging pulse show that material from the crater is expelled during the damaging pulse. This material is initially expelled at speeds of about 5×10^6 cm/sec and continues to be expelled more than a microsecond after the damaging pulse. It is mostly emitted normal to the surface. This is apparent in Figure 11 which is a single exposure hologram taken 900 ns after damage initiation.

From this knowledge of the plasma characteristics the following model can be constructed. Within one nanosecond after plasma initiation there is a layer of plasma several wavelengths thick contiguous to the surface of interest. This plasma is densest at its source; that is, next to the surface. The plasma free electron density continues to increase as the plasma expands and the remainder of the damaging pulse impinges upon the system. This density becomes greater than 10^{21}/cm^3 when the energy density in the laser pulse is significantly above threshold. Thus the system in which we

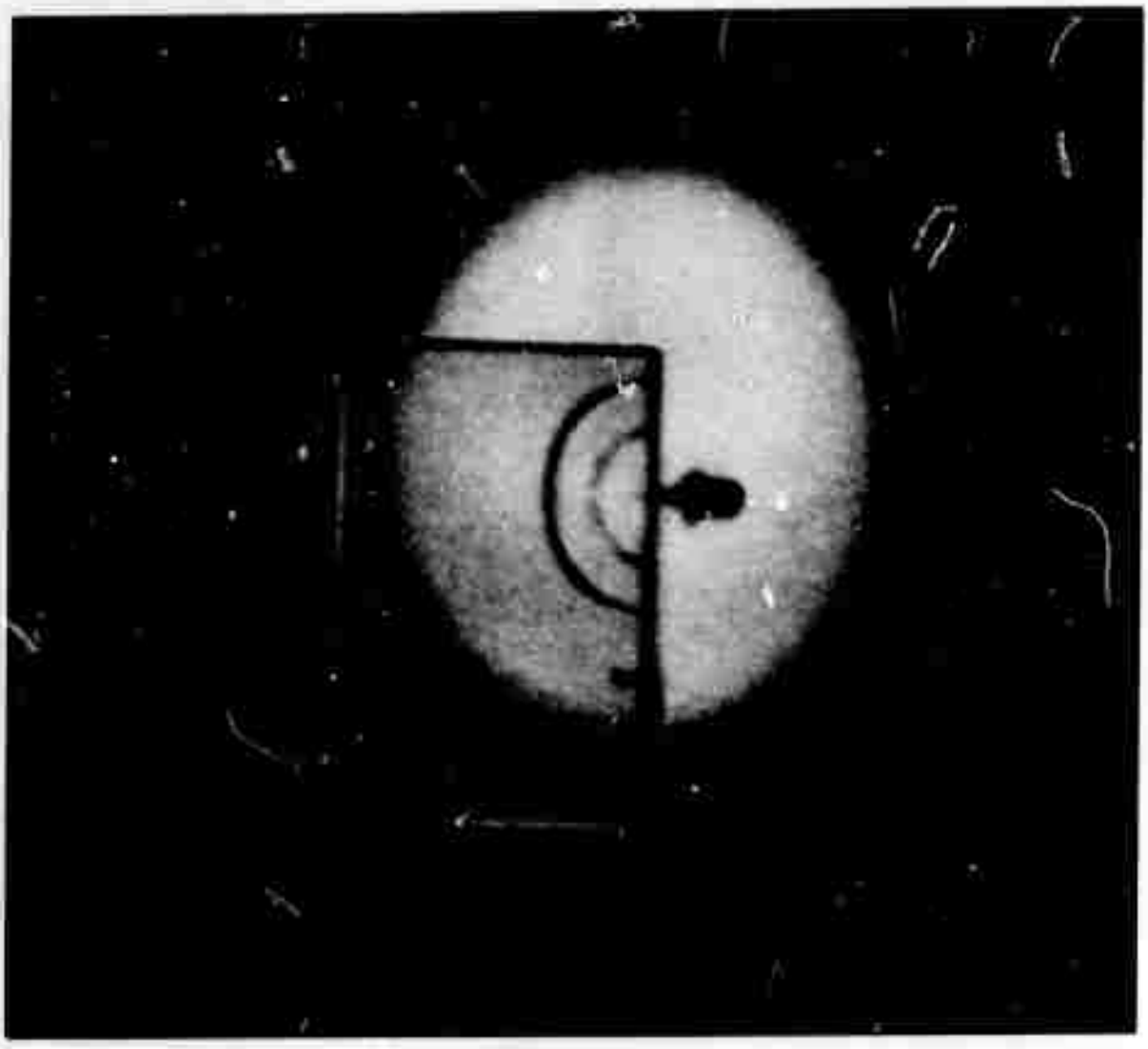

Figure 11 - Damaged cube 900 ns after passage of the damaging pulse.

examine the behavior of the electric field consists of a dielectric surface cover by a deep layer of plasma in which the electron density is increasing in time.

This model can be used to examine the electric fields at the exit face after a laser pulse with energy density well above threshold has initiated a plasma. In Figure 12 E_T and E_R are, respectively, the magnitudes of the electric vectors in the glass of the incident plane wave and the wave reflected from the plasma-glass boundary. The magnitude of the electric vector at the surface is E_{ex}. The index of the refraction of a lossless plasma is given by

$$n_p = \left(\frac{1-\omega_p^2}{\omega^2} \right)^{\frac{1}{2}} \qquad (28)$$

where ω is the angular frequency of the laser pulse and ω_p, the plasma frequency, is approximately $3.6 \times 10^9 N_e$. N_e is the free electron density per cm^3 in the plasma. Note that as the electron density increases from zero to the critical density N_c, $10^{21}/cm^3$ for 1.06 μ radiation, n_p is real and decreases from one to zero. When $N_e > N_c$, n_p is pure imaginary. Knowing how n_p changes with the electron density, Fresnel's equations can be used to examine E_R and E_{ex} (Figure 12) during the laser pulse. The result for E_R is

$$\frac{E_R}{E_T} = \frac{n - n_p}{n_p + n} \quad , \qquad (29)$$

where n is index of refraction of the glass. According to Equation (29), E_R increases as the plasma electron density increases. When $N_e > N_c$ the incident wave is totally reflected. Equation (29) also shows that for $N_e < N_c$ the

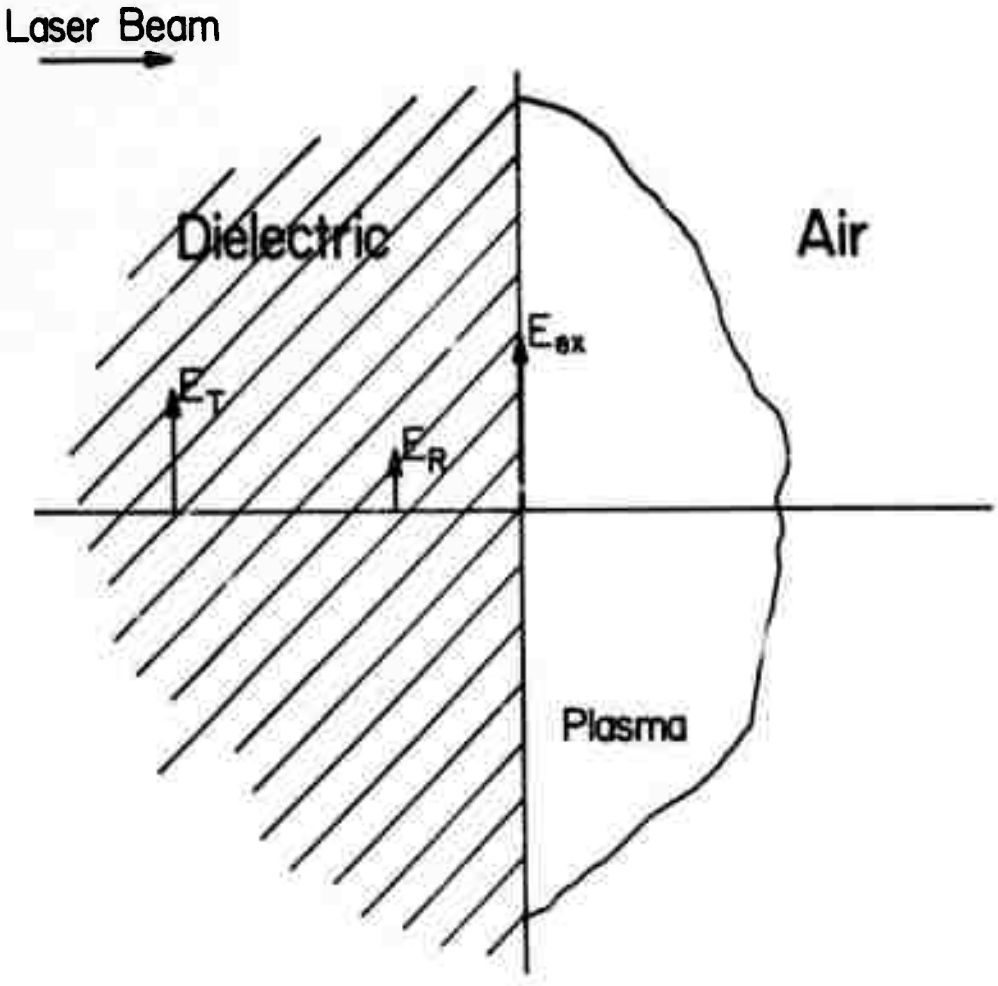

Figure 12 - Exit surface when a plasma is present. The light wave incident on the exit surface has an amplitude $\vec{E}_T$. The reflected wave has an amplitude $\vec{E}_R$ and the resultant wave at the interface is $\vec{E}_{ex}$.

relative phase between E_T and E_R is zero. Another of Fresnel's equations takes this into account and gives

$$E_{ex} = E_T + E_R = \frac{2\,n\,E_T}{n_p + n} \tag{30}$$

As N_e increases toward N_c, E_{ex} approaches $2E_T$. For $N_e < N_c$, E_{ex} is also the magnitude of the electric vector at the antinodes of the standing wave which is formed inside the glass by the incident and reflected waves. This standing wave extends into the glass a distance approximately equal to the coherence length of the laser which is typically less than one mm for neodymium glass lasers with no longitudinal mode control. When $N_e > N_c$ the phase shift between E_T and E_R is no longer zero and E_{ex} is less than $2\,E_T$. However, the incident wave is still totally reflected, so the magnitude of the electric vector at the antinodes is still $2\,E_T$.

In brief, the result of the process described above is that as the plasma density at the exit surface increases a standing wave is formed inside the glass near the surface. The electric field at the antinodes of this standing wave can become twice as large as the electric field in the incident beam. The first antinode is within one quarter wavelength of the surface. It is this large electric field at the antinodes that initiates pitting at or just inside the surface.

After pitting begins the surface is no longer well defined and this simple model does not apply. At this stage absorption is enhanced by the absence of a sharp boundary between the plasma and the glass. The plasma in the initially small pit now rapidly absorbs energy from the laser pulse. The result of this is catastrophic growth of the pit and spallation of material from the surface at the high velocities observed.

Let us now consider the entrance surface. The system shortly after a pulse with power density greater than that of the entrance threshold is shown in Figure 13. The symbols of this figure are the same as in Figure 12, except E_T is replaced by E_I, the electric vector of the laser beam in air and plasma, and E_{ex} is replaced by E_{ent}. It follows from Fresnel's equations that

$$\frac{E_R}{E_I} = \frac{n_p - n}{n_p + n} \tag{31}$$

and

$$\frac{E_{ent.}}{E_I} = \frac{2n_p}{n_p + n} \quad . \tag{32}$$

Equation (31) takes into account the 180° phase reversal of E_R as shown in Figure 11

From Equations (31) and (32) it is seen that E_R approaches E_I and $E_{ent.}$ approaches zero as the plasma electron density increases toward N_c. When $N_e > N_c$ the plasma itself begins to reflect the incident beam. Consequently, as the plasma grows more dense at the entrance face it increasingly shields the surface from the laser beam. However, when losses in the plasma and the smoothly changing index experienced by the laser pulse in going from air to plasma are taken into account, very effective heating of the plasma by the pulse can be expected. The thermal shock that results from the hot plasma spreading over the surface causes the characteristic rippling and cracking on the entrance surface. The absence of a standing wave inside the glass precludes pitting damage of the sort seen at the exit.

Now consider the experimental evidence for the above explanation of the form of damage. The contention that the electric field in the standing wave at the exit surface is responsible for exit pitting is supported qualitatively

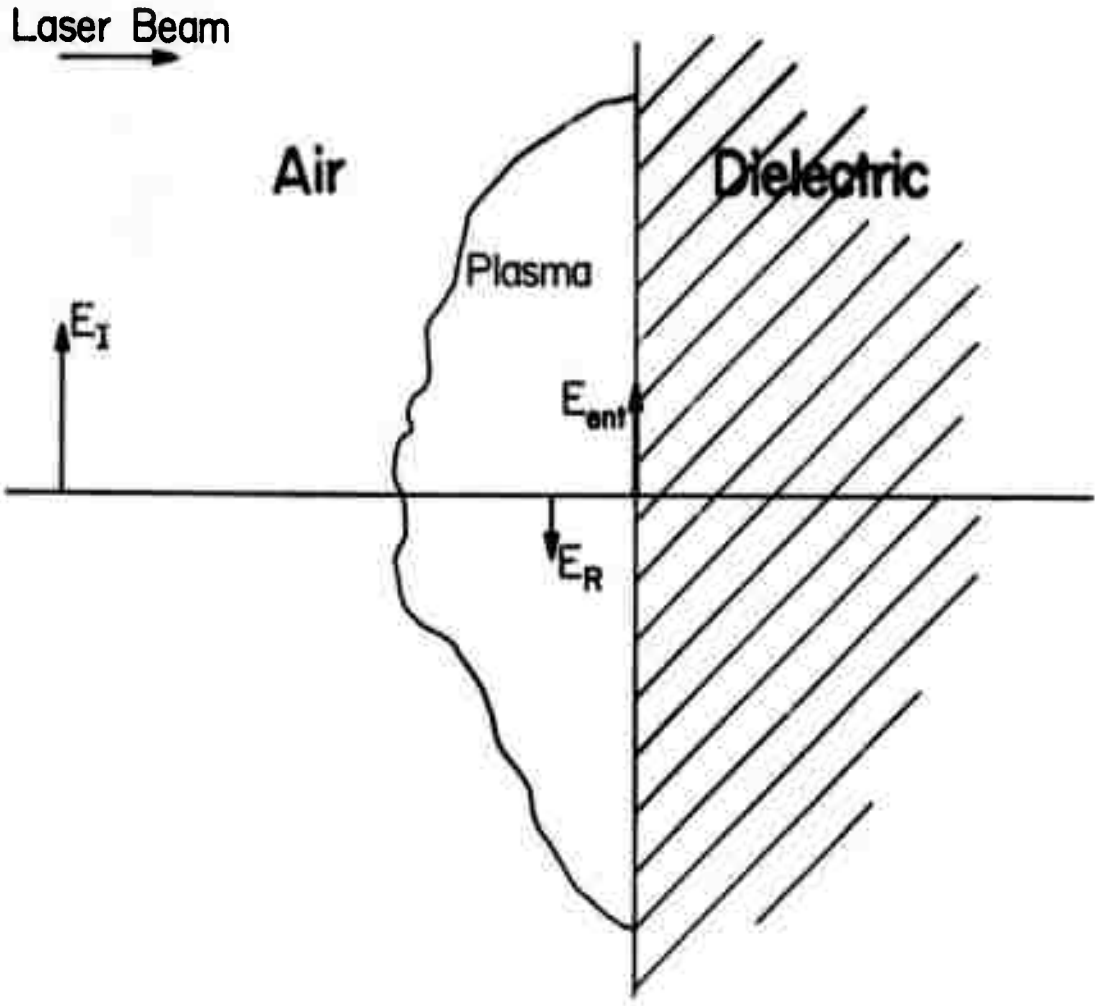

Figure 13 - Electric fields at the entrance face when a plasma is present. The incident electric field is E_I, the reflected electric field E_R and E_{ent} is the resultant field at the interface.

by the fractured appearance of the crater. This fractured appearance and the ejection of glass fragments suggest that the pit is a result of a sub-surface explosion,[3] which is completely consistent with a standing wave just under the surface. The appearance of entrance damage, on the other hand, strongly suggests a phenomenon occurring outside the surface, again in agreement with the model. The fact that no asymmetry in damage form is observed in glass which damages without plasma formation provides still more qualitative evidence.

The model is quantitatively supported by the relative energy densities required for internal and exit surface breakdown. In Owens-Illinois ED-2 laser glass, for example, exit pitting begins to occur at 130-150 joules/cm^2 for a 30 ns pulse, while the internal damage threshold is 400-600 J/cm^2. When the field at an antinode is $2E_T$ for a damaging pulse of 130-150 J/cm^2, the energy density at the antinodes corresponds to 520-600 J/cm^2. In view of this it is perhaps more appropriate to characterize exit pitting as internal damage rather than surface damage. The only difference between the two is that at the surface the fractured glass has some place to go.

Using the proposed model it can be predicted that for a given dielectric, the nearer to unity the ratio of exit plasma threshold to internal damage threshold, the more severe pitting damage will be when it does occur. Thus it is observed that no pitting occurs just above the plasma formation threshold of approximately 100 J/cm^2 in ED-2 glass. Even if the plasma becomes dense enough to totally reflect the beam, the electric field at the antinodes does not become great enough to initiate internal damage. On the other hand, if ED-2, for example, could be treated in such a way as to raise the plasma threshold to 300 J/cm^2, the electric fields at the antinodes would correspond

to 1200 J/cm^2. This is far above the internal threshold and severe pitting would always result, even at the surface threshold. The severity would be compounded by the fact that at high damage thresholds there is more energy in the portion of the pulse incident upon the system after plasma formation. This effect has been observed in studies of ion polished sapphire.[3]

Streak photos of entrance plasmas taken when the laser pulse struck the surface at oblique incidence showed that the plasma has three components: one normal to the surface, one growing into the incident beam and a weak one along the reflected beam.[3] The latter two are extant only during the laser pulse and expand at twice the rate of the normal component, and consequently are hotter than the normal component. When the same experiment was formed in vacuum the two components along the beam vanished. These observations are consistent with the model presented here, according to which the initial source of the plasma is the dielectric surface. After this plasma becomes dense enough to absorb appreciably, the air in the plasma is heated and becomes a secondary plasma source. This source is along the incident and reflected beam. Heating of the air plasma is facilitated by the absence of a sharp boundary between the surface plasma and the air. When the exit surface plasma was examined in Reference 3 only a normal component was observed in either air or vacuum. This component expanded at the same rate as the normal component at the entrance and thus can be assumed to be at approximately the same temperature. The absence of a non-normal exit component does not seem to be easily explained. Tentatively, one can hypothesize that when the plasma originating from the dielectric face becomes dense enough to absorb appreciably, it is dense enough to cause a large reflection. Consequently, energy sufficient to significantly heat the secondary air source does not reach the region of the plasma along the refracted beam.

The fact that the entrance surface is generally more prone to cracking than the exit is easily explained by the observation of Reference 3 that the entrance plasma is hotter than the exit plasma and thus subjects the entrance to a greater thermal shock.

Further experimental verification of the model presented in this section could be gained by observing increased specular reflection of the damaging pulse from the exit glass-plasma interface. We have looked for such an increase in specular reflection with a detection system capable of responding in less than 0.5 ns and no increase was observed. This is reasonable when one considers the time required for reflection at the plasma-glass boundry to grow from its low value in the absence of the plasma to a very high value and then become diffuse as the surface is violated. Considering the catastrophic nature of the avalanche process leading to the plasma, the time required for N_e to increase from $10^{19}/cm^3$, where enhanced reflection from the plasma is negligible, to $10^{21}/cm^3$ could well be no more than a few pico-seconds. Since electron-lattice collision times are much shorter yet, pitting of the surface, and consequently diffuse reflection, can be expected to occur in the same time regime. This would render increased specular reflection unobservable with the detection system we used. Furthermore, since plasma initiation is localized,[20] the plasma begins in a very small area and grows. This means that unless the beam is sharply focused only a small fraction of the total cross section of the beam is incident on the dense plasma while the surface is still intact, thus rendering the enhanced reflection even more difficult to detect.

It is interesting to speculate on the damage that would be caused by a laser with a coherence length of several millimeters. If such a laser were focused not too sharply on the exit surface, so that the reflected wave could

interfere with the incident wave over a distance of several millimeters, a damage track extending into the dielectric might result. The length of this track would depend upon the time required for the high reflection from the plasma-dielectric boundary to go from specular to diffuse. Since this could be a matter of only a few picoseconds or less, the track would be correspondingly short.

The analysis in this section has implicitly assumed that the damaging pulse is long enough to allow the surface plasma to expand to a thickness of several wavelengths during the latter part of the pulse; that is, the pulse is greater than approximately 1 ns. It is expected that damage from picosecond pulses might exhibit different morphologies than are found in the nanosecond regime.

In summation, reflections at the glass-plasma interfaces lead to a plausible model that explains the observed asymmetry in exit and entrance damage form. Although direct experimental observation of these reflections at the exit may be difficult, their existence follows from basic physical considerations and experimental observation of sufficient plasma density. Finally, the question of whether the plasma is the cause of damage is clarified in the model presented here. The creation of the plasma may not cause significant damage, but the interactions of the remainder of the pulse with the plasma-glass system does.

II-7. CONCLUSIONS

Local electric field strengths are of primary importance in determining surface damage to transparent dielectrics. By considering the local electric field strengths it is now possible to quantitatively explain two well established experimental observations. The first is the asymmetry in the

entrance and exit surface damage thresholds. The second is the drastic reductions in surface damage thresholds caused by scratches or other irregularities on or near the surface.[2] The theoretical explanations for these observations are generally applicable to all transparent dielectrics. Morphological differences in exit and entrance surface damage can also be explained by considering the local electric fields, but here the particular properties of different dielectric materials may play a larger role.

Much is still to be learned about the particular damage mechanisms involved in various materials and for pulses of different duration. For example, it is at present difficult to explain why certain glasses have damage thresholds significantly higher than other glasses, and why certain materials always display a plasma when they are damaged while other materials damage without a plasma. This second observation suggests that the evolution of damage is different for different materials. Study of damage for different polarizations and geometries may show more precisely how the damage threshold depends on local electric fields. Theory also suggests that damage from picosecond pulses could have a different form than damage caused by pulses longer than a nanosecond.

The most promising approach for increasing the surface damage threshold of a given material is to avoid intense local electric fields. For example, multilayer dielectric coatings should be designed with this in mind. Small digs and scratches in the surfaces can also lead to high local fields. Super polishing techniques offer promise of reducing these.

III. THERMODYNAMIC STUDIES

III-1. MELTING STUDIES

The objectives of the experimental melting study during this period were to eliminate oxygen which was evolved from the batch during melting and to use low-high oxygen partial pressure atmosphere cycling during melting for the purpose of redissolving any platinum sparklers which may have formed.

III-1.1 Pretreatment of Batch Materials

The pretreatment of batch materials in order to eliminate oxygen available to the melt was discussed in the last report.[6] Possible sources of oxygen are sorbed water, oxygen, and carbon dioxide, as well as entrapped air. Additional melts to those previously reported are listed in Table 2. These data demonstrate that 0.1 wt.% graphite, 0.25 wt.% silicon monoxide, and 0.15 wt.% silicon could lower the Ce^{+4} content of the glass to an undetectable level (less than 0.005 wt.%).

III-1.2 Low-High Oxygen Partial Pressure Melting

A previous report [21] described experiments in which a glass containing 19,000 sparklers per cubic inch was remelted in a highly oxidized atmosphere in a silica crucible. The sparkler count was decreased to 18. Although this would be a good approach, the glass attacks silica resulting in unacceptable cordy glass. This experiment did show, however, that raising the oxygen partial pressure of the melt increases the solubility of platinum in the laser glass melt causing solution of particulate platinum. In order to be of commercial interest, the concept of keeping sparklers dissolved at a higher oxygen partial pressure would have to be observed in a platinum crucible.

TABLE 2

EFFECT OF ADDITIONS ON THE OXIDATION STATE OF CERIUM*

Additive Material	Wt.%	Crucible Material	Ce_2O_3 Wt.%	CeO_2** Wt.%
Graphite	0.01	Carbon	0.38	0.080
"	0.05	"	0.45	0.024
"	0.10	"	0.47	< 0.005
"	0.15	"	0.47	< 0.005
"	0.20	"	0.46	< 0.005
SiO	0.05	silica	0.34	0.099
"	0.10	"	0.39	0.059
"	0.15	"	0.40	0.016
"	0.20	"	0.46	0.010
"	0.25	"	0.44	< 0.005
"	0.30	"	0.44	< 0.005
"	0.40	"	0.43	< 0.005
"	0.50	"	0.45	< 0.005
"	0.60	"	0.44	< 0.005
"	0.70	"	0.44	< 0.005
Si	0.05	silica	0.41	0.038
"	0.10	"	0.43	0.007
"	0.15	"	0.42	< 0.005
"	0.20	"	0.44	< 0.005
"	0.25	"	0.45	< 0.005

* Melting conditions 2100° for 2 hours in gas fired furnace operating at 4% excess combustables.

**detectability limit for Ce^{+4} is 0.005% CeO_2

Table 3 lists three melts which successfully provided a melting cycle with an initial, reduced oxygen partial pressure followed by an increase (a less reduced) oxygen partial pressure. Based upon the relationship between oxygen partial pressure and platinum solubility, these melts were expected to eliminate platinum sparklers. The occurrence of sparklers in these melts can possibly be explained by a high platinum concentration (caused by a high oxygen content) surface layer of glass being swept into the more reduced, low oxygen content glass within the bulk of the melt. Local regions of the glass may have therefore seen a melting cycle conducive to sparkler formation.

Table 4 lists nine additional melts which were made during this report period. Columns 2, 3, and 4 refer to the batch pretreatment; columns 5, 6, 7, and 8 refer to the melting of the pretreated batch in order to obtain the final glass. Column 2 indicates the Batch Pretreatment and Condition: the weight percent SiO added to the raw batch and the total sample weight are given. After pretreatment, the melt was either poured through water-cooled, stainless steel rollers in order to obtain glass flakes or was poured into a graphite mold in order to form a solid casting. Column 3 estimates the oxygen partial pressure in equilibrium with the bulk glass after pretreatment. The $10^{-6.5}$ atm. value is estimated from the analysis of the Ce^{+3}/Ce^{+4} ratio of the pretreated batch to which smaller additions of SiO were added and from previous laser glass melts (see Figure 1, Reference 5). The 10^{-12} atm. value is also estimated by extrapolation of the same data. The 10^{-21} atm. value is estimated from the discoloration and cloudiness of the glass after pretreatment. The previous thermodynamic study indicated that silicon metal would be the first to precipitate from the melt if the melting conditions were too reduced. The

TABLE 3

LOW-HIGH P_{O_2} MELTS(1)

Melt No.	Batch Weight (grams)	Estimated Equilibrium PO_2 (atm.)(3)	Cover Gas		Pt (ppm)	Sparklers
			Gas	PO_2		
153F	248	$10^{-6.5}$	N_2	10^{-6}	2.22	156
153G	290	$10^{-6.5}$	$H_2/H_2O/A$	$10^{-6.35}$	1.28	232
153H	220	$10^{-6.5}$	O_2/N_2	$10^{-3.5}$	1.93	125,000(4)

(1) Melting conditions: 2600°F - 20 hours, stirred.

(2) Batch was premelted with 0.25 wt% SiO (See Table 1) and rolled into flakes.

(3) See previous semiannual report Fig. 1, page 23.

(4) These sparklers in the form of long rods.

TABLE 4

Melts Made During This Reporting Period

Melt No.	Batch Pretreatment & Condition	Estimated Equilb. P_{O_2}	Color	Melting Time & P_{O_2}	PPM Pt	Sparklers	Remarks
178A	No Pretreatment	High	-	25-1/4 hrs total; 19 1/2 hrs, $10^{-10.35}$; & 5-3/4 hrs, $10^{-6.35}$	0.015	~3000	
153B	0.25 wt.% SiO; casting	$10^{-6.5}$	Blue	25-1/4 hrs. total; 19-1/2 hrs., $10^{-10.35}$; & 5-3/4 hrs., $^{-6.35}$	0.035	150,000	
153C	0.25 wt.% SiO; 2 castings; 264g	$10^{-6.5}$	Blue	19-1/2 hrs; $10^{-10.35}$	0.015	3,000(1000)	
153D	0.25 wt.% SiO; flakes; 214g	$10^{-6.5}$	Blue	19-1/2 hrs: $10^{-6.35}$	0.465	16	No Stirring
153E	0.25 wt.% SiO; casting; 343g	$10^{-6.5}$	Blue	21 1/4 hrs. $10^{-6.35}$	0.105	50,000 (large whiskers)	Cored, not cast
191A	0.5 wt.% SiO; casting; 150g	~10^{-18}	Blue	20 hrs; $10^{-10.35}$	0.027	43	
198A	0.7 wt.% SiO; casting; 110g	~10^{-21}(?)	Red & Clear	20 hrs; $10^{-10.35}$	0.045	640	
205B	1.3 wt.% SiO; casting; 118.29g	~10^{-21}(?)	Cloudy	20 hrs; $10^{-10.35}$	0.35	2010	
205C	1.3 wt.% SiO; casting; 99.5g	10^{-21}(?)	Cloudy	20 hrs; $10^{-10.35}$	3.75	16	No stirring

gray, cloudy melt is believed to contain silicon metal in equilibrium with the melt. As long as silicon metal and SiO_2 (in glass solution) are both present, the oxygen partial pressure is fixed according to the phase rule. Appendix A shows the thermodynamic calculation. Column 5 describes the melting conditions used for converting the pretreated batch to the final product. Column 6 is the analysis of total (dissolved and particulate) platinum. Column 7 gives sparkler count per cubic inch by microscopic examination.

Based upon the experience of previous melts[5], the nine melts were expected to be more successful than actually found. Some pretreatment was expected to give a lower sparkler count than no pretreatment. Raising the oxygen partial pressure at the end of the run was expected to also be more beneficial in reducing the sparkler count than using a constant oxygen partial pressure. Because these melts were not as successful as anticipated, one can only speculate at this time why sparkler counts were higher. In this sense, the semi-annual report is truly a report of research in progress; absolute reasons for findings are not possible with the number of experiments performed. Possible explanations for the high sparkler counts are given below.

Although the melts listed in Table 3 were more successful in achieving an oxygen partial pressure cycle which favors platinum solubility as time increased, melts 178A and 153B were somewhat successful in achieving the desired oxygen partial pressure cycle. It is possible that these melts produced more sparklers than melts 3, 4, and 5 listed in Table 3 of the last report[6] (page 21) for the same reasons given in the discussion of the melts in Table 2; surface glass swept into the bulk glass may have caused an unfavorable oxygen partial pressure cycle and platinum concentration cycle

in local regions of the melt. Note that 5-3/4 hours at an oxygen partial pressure of $10^{-6.35}$ atm. did not appreciably increase the total platinum content of melt #178A.

Melts 153B, 153C, and 153E were carried out before the analysis of Ce^{+3}/Ce^{+4} was completed; therefore, the degree of oxidation of the pretreated batch was not known until after the runs were made. An oxidized-reduced cycle was therefore inadvertently obtained which may have also caused the relatively high sparkler count. Again, the 5-3/4 hours at an oxygen partial pressure of $10^{-6.35}$ atm. did not appreciably affect the total platinum content in melt #153D.

The sparkler count in 191A and 198A may have been caused by the original platinum concentration in the original raw materials (approximately 80 ppb), as reported on page 9 of the last report.[5] Additional analyses of the raw materials show that the platinum concentration was higher in the raw materials than in these final melts (30 and 50 ppb). Platinum may have precipitated due to the low oxygen partial pressure of the cycle.

Melts #205B and 205C have unusually high platinum concentration suggesting that very reduced pretreated raw materials may affect platinum solubility precipitation. Possibly crucible attack may increase platinum solubility in the glass as discussed in the last report[5] (pages 4-5). This phenomena is not well understood.

Comparing melts #153D to 153G and 205C to 205B indicate that no stirring may affect the kinetics of sparkler formation; forced stirring of surface glass into the bulk of the melt may not be desirable.

III-1.3 Discussion

The complexity of melting laser glass without platinum sparklers is now well respected. As stated in Reference 5, the solution-precipitation mechanism (previously referred to as the solution-dissolution mechanism) is the most difficult to overcome because of the kinetics of treating the entire bulk of glass. If a relatively low oxygen partial pressure is followed by a still lower oxygen partial pressure during the melting cycle, the precipitation of platinum sparklers occurs as expected from the relationship between oxygen partial pressure and platinum solubility in the glass. If a low oxygen partial pressure is followed by a higher oxygen partial pressure, platinum sparklers are also found. The actual combination of oxygen partial pressures during a melting cycle in order to eliminate sparklers is still elusive.

III-2. DETERMINATION OF ACTIVITIES - EMPIRICAL STUDY

The thermodynamic activities of oxides in laser glass composition #5[22] (a Li_2O-CaO-SiO_2-Nb_2O_3 glass) and of the corresponding metals in platinum were determined through a subcontract to Battelle Memorial Institute, Columbus Laboratories. The results were reported in a previous semi-annual report[21]. Examining the data has indicated some significant inconsistencies.

For the reaction:

Si (pure liquid) → Si (in liquid Pt sol'n)

$\Delta F = RT \ln a_{Si} = \Delta H - T\Delta S$

ΔS should be $S^{\text{ideal mixing}}_{Si \text{ in } Pt} = R \ln X^{Pt}_{Si} + \Delta S$ phase transformation $\simeq +16$ e.u. (calories/mole degree). A plot of RT ln a_{Si} at $P_{O_2} = 10^{-6}$ atm. gives $\Delta S = -7.84$ e.u. Note that the value is not close to the estimated value of +16 e.u. Also note that the entropy for the reaction Si(pure)→ Si (sol'n) cannot be negative.

For the reaction:

Al (pure liquid) → Al (in liquid Pt sol'n)

ΔS must again be positive. A plot of RT ln a_{Al} versus T at $P_{O_2} = 10^{-10}$ atm. gives an entropy of -101 e.u.

The most likely source of error is sample depletion or interaction with the BeO crucible used as the Knudsen cell. It may be appropriate to consider the activities reported on July 31, 1971[21] in Table 3 to be lower limits of the thermodynamic activities. Sample depletion or crucible interaction would have lowered the thermodynamic activities of the metals in the platinum from the activity values actually desired

when the platinum is in equilibrium with the glass. Determining the activities of metals in platinum would have been easier if the solute metals existed in the platinum in greater concentrations than the parts per million concentration actually found.

III-3. REVIEW OF RESEARCH DURING THE PERIOD JULY, 1970 TO JULY, 1972

The goal of this research was the elimination of platinum sparklers formed during the melting of laser glass, at least to the extent that they are no longer of appreciable concern as damaging sites. The study is predicated on the assumption that oxygen in the melting environment is necessarily involved in producing platinum sparklers in the finished glass; certainly the variations of sparkler count and of total (dissolved and particulate) platinum found during the study strongly support this assumption. The oxygen level cannot, however, be reduced arbitrarily since attack of the platinum crucible by oxides composing the glass occurs below a certain partial pressure of oxygen. Consequently, the first phase of the work consisted of a thermodynamic study of laser glass in platinum. By determining the activities of the several oxides present in various laser glass compositions and the activities of the corresponding metals in platinum, the minimum partial pressure of oxygen which must be maintained in order to prevent crucible attack was determined to be 10^{-12} atm. Subsequent research consisted of reducing to practice the results obtained in the thermodynamic study in order to eliminate platinum sparklers as damage sites.

Highlights of the research performed under the contract follows:

1. A comprehensive literature search of the activities of oxides in several laser glasses and of the activities of corresponding metals in platinum has been compiled.[5-21]
2. The literature review was used in order to estimate the thermodynamic activities of interest.[5,21]

3. Consideration of several theoretical models available from the literature indicated that the thermodynamic activities could not be predicted to within two orders of magnitude.[5,21]

4. Subcontracted experimental research performed by Battelle Memorial Institute of Columbus, Ohio has fixed limits on the thermodynamic activities of interest.[21],*

5. Batch pretreatment using SiO, Si, and C has been successful in eliminating oxygen from the initial laser glass batch materials.

6. The partial pressure of oxygen above the laser glass melt and the partial pressure of oxygen in equilibrium with the bulk melt have been found to be dramatic parameters controlling the total platinum content of the laser glass and the occurrence of platinum sparklers.[5],*

7. Using partial pressures of oxygen of 10^{-10} atm., laser glass was melted in platinum with the resultant platinum content of .017ppm.

8. The sparkler count within a laser glass sample was decreased from 19,000 sparklers per cubic inch to 18 sparklers per cubic inch by remelting the sample in a more oxidizing atmosphere than previously used.[5]

9. An important mechanism for the occurrence of platinum sparklers in laser glass was found to be the Solution-Precipitation mechanism. The platinum dissolves in the glass as an oxide or as an oxide

*Footnote: Also see this Report

complex. The platinum either remains dissolved or is precipitated as platinum sparklers depending upon the difference in oxygen partial pressure between the initial and final melting stages.[5],*

10. Buffer gases (CO/CO_2 and H_2/H_2O) were effectively used in order to control the oxygen partial pressure above the melt and in order to change the oxygen partial pressure in equilibrium with the bulk melt, as evidenced by the Ce^{+3}/Ce^{+4} and by total platinum content analyses.[5],*

11. Although the partial pressure of oxygen above the laser glass melt and the partial pressure of oxygen in equilibrium with the bulk melt strongly affect the occurrence of platinum sparklers, a laser glass melt within a controlled oxygen environment has not been made with zero platinum sparklers to date.[5],*

---

*Also see this Report.

IV. REFERENCES

1. M. D. Crisp, N. L. Boling and G. Dube, to be published in Appl. Phys. Letters, October 15, 1972.
2. N. Bloembergen, submitted to Applied Optics.
3. C. R. Guiliano, R. W. Hellwarth and G. R. Rickel, Semiannual Report 5, ARPA Order No. 1434, January 1972.
4. N. L. Boling, G. Dube and M. D. Crisp, to be published in Applied Physics Letters, November 15, 1972.
5. N. L. Boling, L. Spanoudis and P. R. Wengert, Damage Threshold Studies of Glass Laser Materials, Semiannual Technical Report, ARPA Order No. 1441, December 1971.
6. R. W. Beck, Damage Threshold Studies in Glass, Semiannual Technical Report, 31 July 1970, ARPA Order No. 1441.
7. M. Bass and H. H. Barrett, Journal of Quantum Electronics QE-8, 338 (1972).
8. C. R. Giuliano, Appl. Phys. Letters 5, 137 (1964).
9. I. A. Fersman and L. D. Khazov, Soviet Physics - Technical Physics 15, 834 (1970).
10. M. Born and E. Wolf, Principles of Optics (Macmillan, New York, 1964), p. 38 ff.
11. V. V. Lyubimov, I. A. Fersman and L. D. Khazov, Soviet Journal of Quantum Electronics 1, 201 (1971).
12. M. D. Crisp, to be published in Optics Communications.
13. W. Haller and N. N. Winogradoff, J. Am. Ceram. Soc. 54, 314 (1971).
14. N. Goldblatt, Appl. Opt. 8, 1559 (1969).
15. E. L. Kerr, IEEE Journal of Quantum Electronics QE-8, 722 (1972).

16. J. M. Dawson, Phys. Fluids 7, 981 (1964).

17. M. Bass, H. H. Barrett and L. H. Holoway, Jr., Scientific Report No. 1, ARPA Contract No. F19628-70-C-0223, ARPA Order No. 1434 AMD #1, February 1972.

18. N. L. Boling and R. W. Beck, "Glass Damage Threshold Studies". ASTM Special Technical Publication 356, 1971, Eds. A. J. Glass and A. Guenther.

19. H. Dupont, A. Donzeland J. Ernest, Appl. Phys. Letters 11, 271 (1967).

20. E. Yablonovitch and N. Bloembergen, submitted to Phys. Rev. Letters, 1972.

21. N. L. Boling, L. Spanoudis and P. R. Wengert, Damage Threshold Studies of Glass Laser Materials, Semi-Annual Technical Report, ARPA Order No. 1441, July 31, 1971.

22. N. L. Boling, L. Spanoudis and P. R. Wengert, Damage Threshold Studies of Glass Laser Materials, Semi-Annual Technical Report, ARPA Order No. 1441, January 1, 1971.

23. JANAF Thermochemical Tables, Office of Standard Reference Data, National Bureau of Standards, available from the Superintendent of Documents, U.S. Government Printing Office, Washington, D. C., June, 1971.

V. APPENDIX A

For the reaction:

$$Si \text{ (pure liquid)} + O_2 \text{ (gas)} \rightarrow SiO_2 \text{ (in glass solution)},$$

$$\Delta F^\circ_{rx} = - RT \ln (a_{SiO_2}/P_{O_2})$$

$$P_{O_2} = a_{SiO_2} \exp (\Delta F^\circ_{rx}/RT)$$

$\Delta F^\circ_{rx} = \Delta F^\circ_f (SiO_2) = -145{,}611$ Calories at 1700°K (Ref. 23)

$a^{glass}_{SiO_2}$ 0.3 (Ref. 21, page 56)

$a^{pure}_{Si} = 1.0$

$P_{O_2} = 6X10^{-21}$ atm.

The above calculation is based upon Si precipitating in glass which is descriptive of the actual system being discussed. When considering Si attacking platinum, $a_{Si} \neq 1.0$ and the P_{O_2} change accordingly.